

# The ESCRT machinery mediates polarization of fibroblasts through regulation of myosin light chain

Viola Hélène Lobert<sup>1,2,3</sup> and Harald Stenmark<sup>1,2,3,\*</sup>

<sup>1</sup>Centre for Cancer Biomedicine, Faculty of Medicine, University of Oslo, 0316 Oslo, Norway

<sup>2</sup>Department of Biochemistry, Institute for Cancer Research, Oslo University Hospital, Montebello 0310, Oslo, Norway

<sup>3</sup>Institute for Cancer Research and Molecular Medicine, Norwegian University of Science and Technology, 7005 Trondheim, Norway

\*Author for correspondence (stenmark@ulrik.uio.no)

Accepted 7 July 2011

Journal of Cell Science 125, 29–36

© 2012. Published by The Company of Biologists Ltd

doi: 10.1242/jcs.088310

## Summary

Recent evidence implicates the endosomal sorting complex required for transport (ESCRT) in the regulation of epithelial polarity in *Drosophila melanogaster*, but the mechanisms responsible for this action remain unclear. Here we show that ESCRTs determine cell orientation during directed migration in human fibroblasts. We find that endosomal retention of  $\alpha 5 \beta 1$  integrin and its downstream signaling effector Src in ESCRT-depleted cells is accompanied by the failure to activate myosin light chain kinase (MLCK), which thereby cannot phosphorylate myosin regulatory light chain (MRLC). Using this mechanism, ESCRT-depleted fibroblasts fail to orient their Golgi complex to undergo directional migration and show impaired focal adhesion turnover and increased spreading on fibronectin. Consistent with these findings, expression of a phosphomimetic mutant of MRLC in ESCRT-depleted cells restores normal phenotypes during cell spreading and orientation of the Golgi. These results suggest that, through their role in regulating integrin trafficking, ESCRTs regulate phosphorylation of MRLC and, subsequently, Golgi orientation and cell spreading.

**Key words:** Adhesion, ESCRT, Integrin, Polarity, MLCK, MRLC, Src

## Introduction

The ability of cells to polarize in order to undergo directional migration is essential to many developmental and physiological processes. However, the mechanisms that orchestrate cell polarization and migration are still not fully understood. The endosomal sorting complex required for transport (ESCRT) has been associated with the regulation of cell migration (Chanut-Delalande et al., 2010; Chanut-Delalande et al., 2007; Lobert et al., 2010; Sevrioukov et al., 2005; Tu et al., 2010). This machinery recognizes ubiquitylated receptors and attenuates their signaling by sorting them into multivesicular endosomes, thereby committing them to lysosomal degradation. Recent evidence also implicates ESCRTs in regulation of epithelial polarity in *Drosophila melanogaster* (Moberg et al., 2005; Thompson et al., 2005; Vaccari and Bilder, 2005). Although the mechanisms by which the ESCRT machinery regulates cell migration and polarity remain unclear, further insight into this issue might provide important clues about how cell polarization is coordinated with membrane trafficking during directional cell migration.

Adhesion sites include focal adhesions (FAs), fibrillar adhesions, focal complexes and podosomes. FAs are stable structures that tend to inhibit cell migration and are located at the cell periphery. Adhesion turnover is characterized by adhesion assembly and disassembly. Adhesion assembly has been well characterized, and requires actin, actin-binding proteins, integrins and Rho GTPases (Webb et al., 2002). Adhesion disassembly is most prominent at the cell rear, where contractility promotes tail retraction (Crowley and Horwitz, 1995). Actomyosin contractility is an important regulator of FA turnover, and myosin II activity is regulated by phosphorylation of the regulatory light chain, myosin regulatory light chain (MRLC).

Although many kinases can phosphorylate MRLC, Rho-associated kinase (ROCK) and myosin light chain kinase (MLCK) are the major kinases responsible for this modification. ROCK regulates MRLC phosphorylation in the cell centre (Totsukawa et al., 2004) and is, therefore, not a major contributor to cell spreading (Betapudi et al., 2006). By contrast, MLCK activates MRLC in the cell periphery (Totsukawa et al., 2004) and regulates integrin-mediated survival signals (Connell and Helfman, 2006). MRLC also plays a role in positioning of the nucleus during cell migration, and the small GTPase Cdc42 activates myotonic dystrophy kinase-related Cdc42-binding kinase (MRCK). MRCK directly phosphorylates MRLC, and controls positioning of the nucleus in relation to the microtubule organization centre (MTOC), which remains immobile (Gomes et al., 2005).

Given that contractility is so central to cell migration, we have investigated whether ESCRTs regulate myosin functions. We show that ESCRTs regulate MRLC by acting on the myosin light chain kinase MLCK through activation of the tyrosine kinase Src, presumably downstream of integrin activation. Through this mechanism, ESCRTs regulate several aspects of cell migration, namely cell spreading, turnover of focal adhesions and fibroblast polarization.

## Results and Discussion

### ESCRT regulates reorientation of the Golgi and of actin fibers during cell migration

Four ESCRT complexes have been characterized to date: ESCRT-0, -I, -II and -III. In order to disrupt ESCRT functions, we targeted the ESCRT-0 component HRS, the ESCRT-I

component TSG101, the ESCRT-II component VPS22 or the ESCRT-III component VPS24 by siRNA. As shown in Fig. 1A, the siRNA molecules led to a considerable reduction in expression of all ESCRT components in BJ fibroblasts. To study fibroblast polarization after monolayer wounding, we used the Golgi as a marker, because it reorients rapidly between the nucleus and the leading edge during directed cell migration (Kupfer et al., 1982). Confluent cell monolayers were starved of serum for 24 hours, wounded and stimulated with serum for 2 hours. Cell polarization was determined by previously described criteria (Bisel et al., 2008; Etienne-Manneville and Hall, 2001; Gomes et al., 2005). Following serum stimulation, we observed an orientation score of 72% in control cells, showing that polarization strongly increased in response to the wound. Interestingly, the orientation score was greatly decreased to a value of 50% in ESCRT-depleted cells (Fig. 1B, C), indicating that ESCRTs play an important role in wound-induced fibroblast polarization. This concurs with the observation that ESCRT-depleted cells showed decreased migration (Fig. 1E; supplementary material Fig. S1) and persistence (the straightness of the cell track) (Fig. 1F), because cells unable to orient are presumably incapable of undergoing directed cell migration. These results are consistent with recent evidence implicating TSG101 in the regulation of cell migration in mouse embryonic fibroblasts (Tu et al., 2010).

The mechanisms that govern reorientation of the Golgi towards the wound before cell migration are not well understood. The function of the Golgi in this position is thought to entail delivery of Golgi-derived vesicles to the newly formed leading edge (Abercrombie et al., 1970; Hay, 1981; Izzard and Lochner, 1980; Kupfer et al., 1982). Organization of the Golgi is maintained by actin filaments (Valderrama et al., 1998), and actin is also required for protein transport to the plasma membrane as well as retrograde transport to the endoplasmic reticulum (Valderrama et al., 2001). Therefore, we investigated how actin fibers oriented themselves in wound healing experiments, especially because the ESCRT-I protein vps28 and the ESCRT-III regulator vps4 have been linked to actin dynamics in *Drosophila* (Rodahl et al., 2009; Sevrioukov et al., 2005). Interestingly, ESCRT-depleted cells were unable to orient their actin fibers towards the wound (Fig. 1B). Cells remained parallel to the wound and were unable to orient themselves perpendicularly to the wound. This could be quantified by actin fiber orientation, which was greatly reduced from 75 to 50% upon ESCRT depletion, suggesting that actin dynamics are regulated by ESCRTs (Fig. 1D). As defects in Golgi reorientation and actin fiber orientation were detected for ESCRT components of different complexes, this suggests that the phenotypes observed occur as a result of a lack of endosomal sorting and not because of other ESCRT functions.

### ESCRTs regulate vinculin localization and cell spreading

Cell adhesion is an important aspect of cell migration because it stabilizes protrusions at the leading edge of the cell and allows contraction of the cell on a substrate (Hynes, 1992). Fibroblasts were trypsinized and replated on coverslips coated in fibronectin. As vinculin is a key regulator of FAs, we co-stained the cells for vinculin and actin. Interestingly, we observed a disorganized cytoskeleton upon depletion of the ESCRT machinery, visible by the staining of actin (Fig. 2A). Additionally, we observed a strong increase in the number of FAs, as well as a different distribution of vinculin staining in control versus ESCRT-depleted cells. In fact, although control cells showed vinculin staining at the tips of the

cells, ESCRT-depleted cells showed an accumulation of vinculin structures all over the cell, consistently capping the actin fibers (Fig. 2A). Importantly, the accumulation of vinculin structures was not accompanied by any increase at the protein level, suggesting that it is the recruitment of vinculin to FAs that was affected (Fig. 2B). We observed that surface area of the cells was increased by 60, 52, 40 and 34% in HRS-, TSG101-, VPS22- and VPS24-depleted cells, respectively (Fig. 2C). Vinculin is classified as a suppressor of cell migration, and vinculin<sup>-/-</sup> mice show a decrease in cell spreading, have fewer FAs and have an increase in cell motility (Coll et al., 1995). Therefore, an increase in FAs and cell spreading and a decrease in cell velocity upon ESCRT depletion [(Fig. 1E; supplementary material Fig. S1) (Tu et al., 2010)] are consistent with ESCRTs being positive regulators of cell migration. Increased cell migration in cells derived from vinculin knockout mice has been attributed to an increase in FA turnover (Saunders et al., 2006), as vinculin is thought to stabilize FAs. Our results are consistent with these findings, and provide a mechanistic link between ESCRT functions and cell adhesion.

### ESCRTs are required for FA turnover

Having observed the strong recruitment of vinculin to FAs, we next investigated whether FA turnover was affected during ESCRT depletion. Considering that the depletion of key subunits from several ESCRT complexes results in a more complete phenotype than single depletions (Stuffers et al., 2009), we depleted HRS and TSG101 simultaneously (Fig. 3C). We investigated assembly and disassembly rates of FAs by performing live cell confocal time-lapse microscopy in cells transfected with a vector encoding TagRFP-vinculin, whose ESCRT machinery had been depleted (Fig. 3A). Interestingly, the rate constants in ESCRT-depleted cells were much lower than in cells transfected with control siRNA (Fig. 3B). These results provide a mechanism by which ESCRT depletion can be linked to decreased cell migration through arrested turnover of FAs. This result is in accordance with the fact that a general decrease in cell velocity is observed in ESCRT-depleted cells [(Fig. 1E; supplementary material Fig. S1) (Tu et al., 2010)], and is accompanied by an accumulation of focal adhesions (Fig. 2A).

### ESCRTs positively regulate myosin light chain functions through MRLC

Given that contractility regulates all the phenotypes presented in this study (fibroblast polarity, cell adhesion, FA turnover), we next investigated whether myosin regulation was affected upon depletion of the ESCRT machinery. Indeed, it has been suggested that MRLC phosphorylation modulates inside-out signaling, namely cell spreading and cell migration (Totsukawa et al., 2004). Importantly, the levels of phosphorylated MRLC were found to be strongly downregulated in ESCRT-depleted cells, whereas levels of total MRLC remained unchanged (Fig. 4A) – this is quantified in Fig. 4B. The observed increase in cell spreading (Fig. 2A,B) fits well with a decrease in actomyosin contractility, because MRLC needs to be downregulated to allow cell spreading, either through the RhoA–ROCK pathway (Arthur and Burridge, 2001; Arthur et al., 2000; Bhadriraju et al., 2007) or through MLCK (Takizawa et al., 2007). Contractility is also required for the positioning of the nucleus during directed cell migration (Gomes et al., 2005), and a decrease concurs with the observed decrease in orientation of the Golgi towards the wound. Finally, contractility

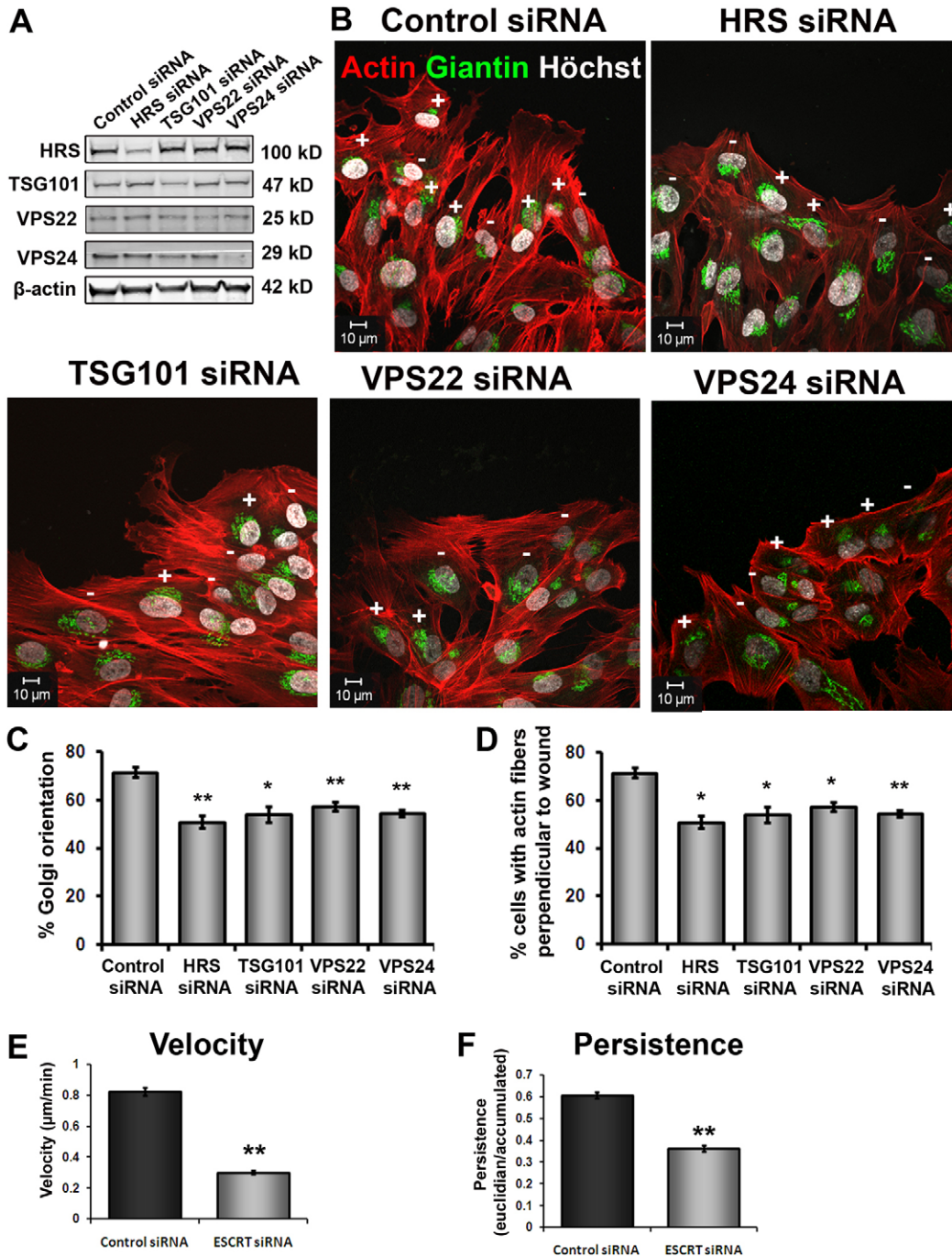


**Fig. 1. ESCRTs are required for polarity and actin fiber orientation during directed fibroblast migration.** (A) Western blotting of control and ESCRT-depleted BJ cells showing the depletion of ESCRT-0 protein HRS, ESCRT-I protein TSG101, ESCRT-II protein VPS22 and ESCRT-III protein VPS24.

(B) Control and ESCRT-depleted confluent monolayers of BJ fibroblasts were serum-starved for 24 hours, wounded and left to migrate for 2 hours in 10% serum. Cells were fixed and permeabilized, stained with antibodies against the Golgi marker giantin (green), and actin (red), and the nuclei were visualized using Hoechst (white). The Golgi was labeled as '+' if its majority lay within a  $120^\circ$  angle facing the wound, and labeled with '-' if not. In each picture, the wound is at the top of the image. Scale bars: 10  $\mu$ m. (C) Quantification of Golgi orientation towards the wound. An average of 74 cells was quantified per condition, per experiment. The graph shows mean values of three independent experiments ( $\pm$  s.e.m.). \* $P < 0.05$ , \*\* $P < 0.01$ . (D) Quantification of actin fiber orientation towards the wound. An average of 50 cells was quantified per condition, per experiment. The graph shows mean values of three independent experiments ( $\pm$  s.e.m.). \* $P < 0.05$ , \*\* $P < 0.01$ . (E) Velocity and (F) persistence (calculated by dividing the euclidean distance by the accumulated distance of the cell trajectories) of control and ESCRT (HRS and TSG101)-depleted BJ cells were determined using Image J software by tracking individual cells during wound healing. Cells were observed for a period of 10 hours. An average of 40 cells per condition and per experiment was assessed. \*\* $P < 0.001$ .



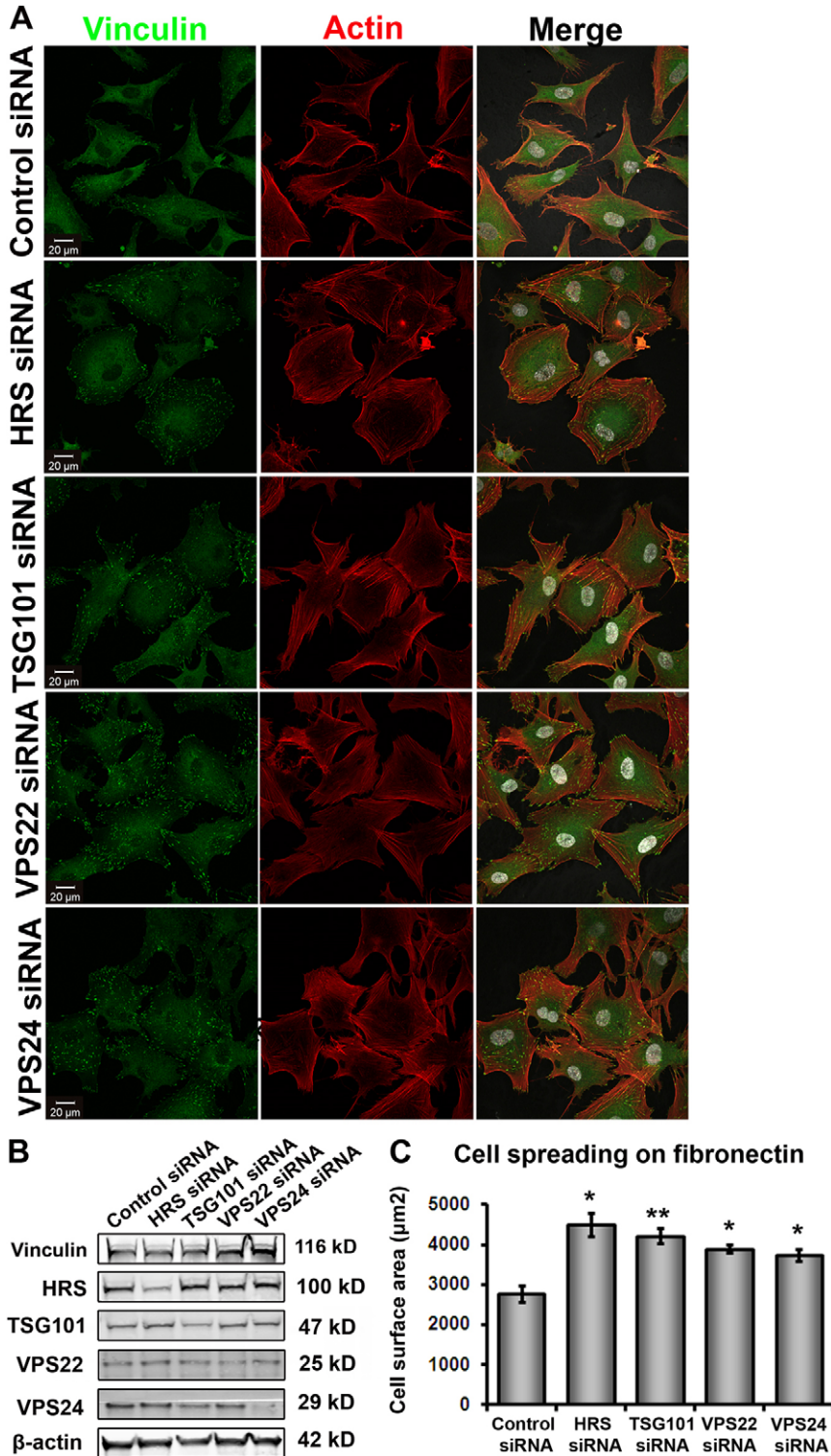


**Fig. 2. ESCRTs negatively regulate cell spreading.** (A) Control and ESCRT-depleted cells were seeded on fibronectin-coated coverslips and left to adhere for a period of 90 minutes. Cells were fixed and stained with antibodies against vinculin and actin. Representative pictures are presented here. Scale bars: 20  $\mu$ m. (B) The cell surface area from cells in A was quantified. An average of 52 cells per condition and per experiment was quantified. Error bars represent  $\pm$  s.e. of three independent experiments. \* $P$ <0.05, \*\* $P$ <0.01. (C) Western blotting of control and ESCRT-depleted BJ cells showing that vinculin expression is not affected by ESCRT depletion, but only its localization as seen in A.

drives disassembly of adhesion (Crowley and Horwitz, 1995) and a decrease in contractility would, therefore, result in decreased FA turnover, as observed (Fig. 3A,B).

In order to determine whether the phosphorylation status of MRLC was directly responsible for the phenotypes observed upon ESCRT depletion, we transfected fibroblasts with a plasmid encoding a phosphomimetic mutant of MRLC (MRLC<sup>EE</sup>).

Strikingly, we observed a decrease in cell spreading (Fig. 4D), an organized actin cytoskeleton, as well as small FAs upon expression of MRLC<sup>EE</sup> (Fig. 4C). This constitutes a virtually complete rescue of the normal fibroblast phenotype, compared with the phenotype observed upon ESCRT depletion. Next, we tested whether MRLC<sup>EE</sup> could rescue the ability of ESCRT-depleted cells to orient towards the wound. Importantly, transfected cells showed a

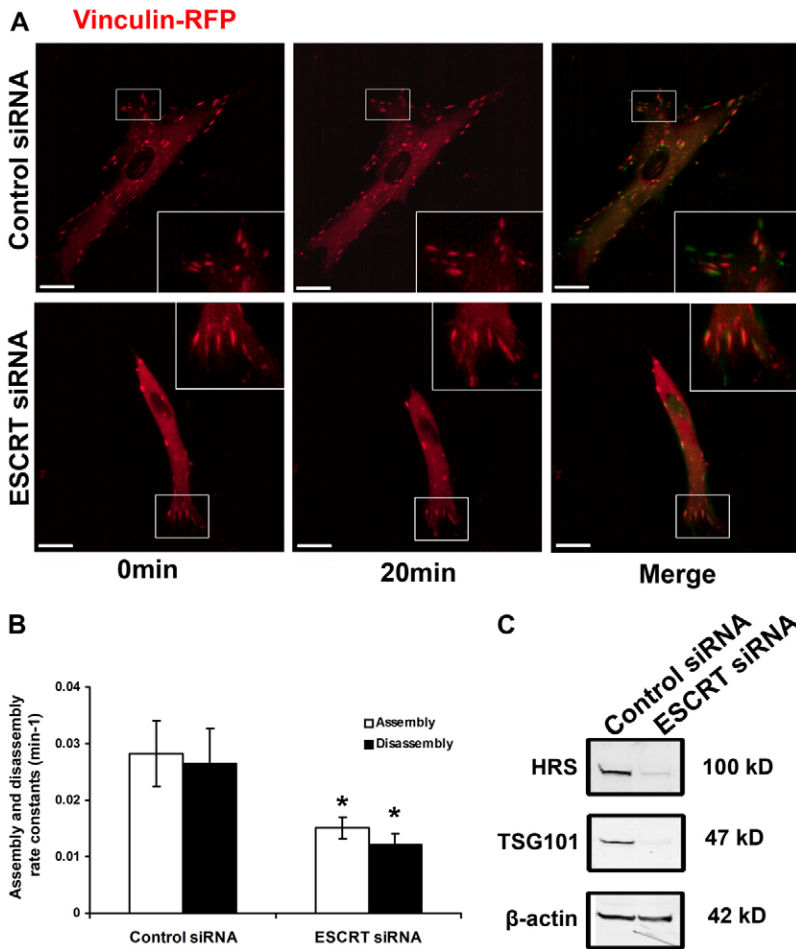


**Fig. 3. ESCRTs are required for turnover of focal adhesions.** (A) Live-cell imaging of TagRFP-vinculin-transfected fibroblasts in the absence or presence of ESCRT depletion. In the merged picture, the red color represents the picture taken at 0 minutes, whereas the green superimposed image corresponds to the picture taken after 20 minutes. The images represent maximum-intensity projections of Z stacks, using Imaris software. Insets show examples of regions with focal adhesions. Scale bars: 20  $\mu$ m. (B) Quantification of assembly and disassembly rates of turnover of adhesion sites from live-cell time-lapse recordings of cells transfected with a plasmid encoding vinculin. Quantifications represent the mean of 30 adhesion sites in seven cells, per condition and per experiment. \* $P < 0.05$ . (C) Western blotting showing that HRS and TSG101 are successfully depleted together.

complete rescue of orientation, and their Golgi were within an area of 120° facing the wound (Fig. 4E,F). This suggests that ESCRTs also regulate Golgi orientation through the regulation of MRLC. Collectively, our results suggest that ESCRTs regulate cell spreading, vinculin localization and Golgi orientation by controlling MRLC phosphorylation.

#### MLCK, an activator of MRLC, is controlled by ESCRTs

The phosphorylation of MRLC is regulated by >12 kinases, with ROCK and MLCK being the main regulators (Vicente-Manzanares et al., 2009). Considering that MLCK regulates MRLC phosphorylation at the cell periphery (Totsukawa et al., 2004), and inhibition of MLCK results in phenotypes similar to those observed upon ESCRT depletion, such as reduced cell migration, reduced persistence, accumulation of vinculin-positive FAs, we investigated the activation status of MLCK upon ESCRT depletion. We observed that phosphorylation of MLCK at tyrosine Y471 was strongly reduced upon depletion of the different ESCRT components (Fig. 4G). This shows that MLCK activity is regulated by ESCRTs, and provides a plausible explanation for the lack of MRLC phosphorylation in ESCRT-depleted cells.

#### Integrin and activated Src accumulate on early endosomes in ESCRT-depleted cells

Phosphorylation of MLCK at Y471 is mediated by Src (Huvencuers and Danen, 2009), which was recently found to

accumulate at late endosomes and lysosomes upon TSG101 depletion in mouse embryonic fibroblasts (Tu et al., 2010). Integrin engagement induces autophosphorylation of focal adhesion kinase (FAK) at Y397, creating a binding site for Src, which subsequently phosphorylates and fully activates FAK (Mitra et al., 2005). FAK Y397 levels are reduced upon TSG101 depletion (Tu et al., 2010), suggesting that integrins might be unable to activate their downstream signaling through FAK and Src in the absence of proper ESCRT functions. We have previously shown that integrin trafficking is regulated by the ESCRT machinery and that integrins accumulate intracellularly upon ESCRT depletion (Lobert et al., 2010). To test the hypothesis that integrin and activated Src accumulate in the same endosomes, we co-stained ESCRT-depleted cells with antibodies against  $\alpha 5$ -integrin and Src Y416-P, together with the early endosome antigen 1 (EEA1) protein. Indeed, integrin and Src-P were found to colocalize strongly at enlarged early endosomes (Fig. 4H), which might represent clusters of vesicles, as observed by electron microscopy (Lobert et al., 2010). Therefore, we propose that, upon ESCRT depletion, Src-P is unable to mediate signaling downstream of integrin owing to its retention in endosomes.

The accumulation of integrin and Src-P at enlarged endosomes suggests that they might be trafficked together. This raises the question of whether Src is downregulated by the ESCRT machinery. c-Src is ubiquitinated by the ubiquitin ligase Cbl-c

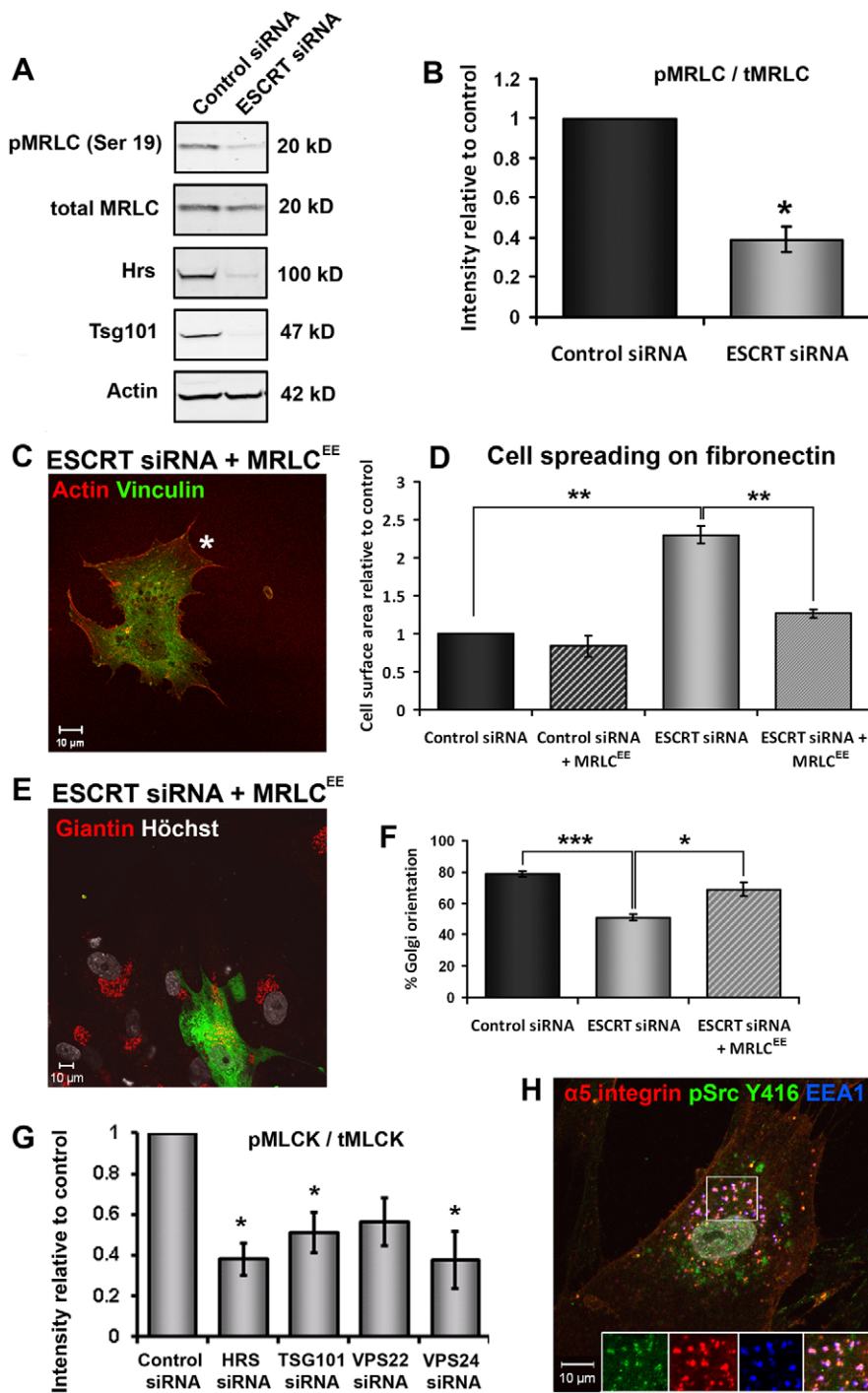


**Fig. 4. ESCRTs regulate myosin light chain functions in fibroblasts through MLCK.**

(A) Western blotting of control and ESCRT-depleted BJ cells showing a decrease in MRLC-*P* (Ser 19). (B) Quantification of phospho- and total MRLC levels in control and ESCRT-depleted cells. Quantifications are based on three independent siRNA and western blotting experiments, and were determined using Odyssey Software (Olympus). Error bars represent  $\pm$  s.e. of three experiments. \* $P$ <0.05. (C) Phosphomimetic MRLC<sup>EE</sup> was transfected into control or ESCRT-depleted cells, and cell spreading experiments were performed as described in materials and methods. The transfected cell is indicated by \*. Scale bar: 10  $\mu$ m. (D) Quantification of cells prepared as in C. Error bars represent  $\pm$  s.e. of three experiments. An average of ten cells was assessed per condition and per experiment. \*\* $P$ <0.01. (E) Phosphomimetic MRLC<sup>EE</sup> was transfected into control and ESCRT-depleted cells before wound healing experiments. Cells were fixed and stained with antibodies against giantin. The transfected cell is visible by its GFP fluorescence. Scale bar: 10  $\mu$ m. (F) Quantification of cells prepared in E. Error bars represent  $\pm$  s.e. of three experiments. An average of ten cells was assessed per condition and per experiment. \*\*\* $P$ <0.0001, \* $P$ <0.05. (G) Phosphorylated Y461 MLCK levels were detected in siRNA-transfected cells by immunoprecipitating MLCK and immunoblotting against phosphorylated MLCK. Levels were normalized to total MLCK levels. The intensity of bands was quantified using the Odyssey software (Olympus), and results are based on three independent siRNA and immunoprecipitation experiments. \* $P$ <0.05. (H) Cells depleted of ESCRTs by siRNA were stained with antibodies against  $\alpha$ 5-integrin, Src Y416-*P* and EEA1. Scale bar: 10  $\mu$ m.

(Yokouchi et al., 2001) and is reported to be degraded by the proteasome (Hakak and Martin, 1999; Harris et al., 1999). Likewise, v-Src is ubiquitinated by Cbl-c but is targeted for lysosomal degradation (Kim et al., 2004). Interestingly, the Src-family kinase Hck and the non-receptor tyrosine kinase Syk are degraded in part by the lysosome (Howlett and Robbins, 2002; Paolini et al., 2001), demonstrating the feasibility of lysosomal degradation of non-receptor tyrosine kinases.

Contractility was recently shown to play a role in vesicle fission at the Golgi (Miserey-Lenkei et al., 2010), thereby

regulating retrograde and anterograde transport. Given that vesicles destined for the leading edge of the cell pinch off the Golgi, and phosphorylation of MRLC is decreased upon ESCRT depletion, it would be interesting to determine whether Rab6 vesicle fission is inhibited upon ESCRT depletion. If so, then this might contribute to the inability of the cells to sense the wound, because delivered products from the Golgi are thought to maintain the leading edge of the cell. The requirement of contractility for fission at the Golgi raises the question of whether myosin II activity is also required at the plasma membrane for vesicle



fission. This could therefore explain slow FA turnover in ESCRT-depleted cells, because adhesion disassembly involves breaking the linkage between integrins and actin.

In conclusion, we propose the following novel mechanism by which ESCRTs regulate cell migration and polarity in fibroblasts: integrins activate FAK–Src upon ligand engagement, causing Src to phosphorylate MLCK, which in turn phosphorylates MRLC, leading to Golgi orientation and FA turnover. ESCRTs are required for the proper trafficking of integrins and Src, because upon depletion of the ESCRT machinery, integrins accumulate at enlarged early endosomes together with activated Src. Activated Src is thereby spatially separated from FAs and is consequently unable to activate MLCK. This, in turn, prevents phosphorylation of MRLC, resulting in decreased FA turnover, increased cell spreading and reduced Golgi orientation.

## Materials and Methods

### RNA interference

siRNA transfection was performed in BJ cells using 75 nM Hrs, 10 nM Tsg101 (Lobert et al., 2010), 25 nM Vps22 (Dharmacon, J-004695-09) and 25 nM Vps24 oligos (sense: AGUGACUGAUGCCCUUCCAGA; antisense: UCUGGAAGG-GCAUCAGUCACU). Transfection was performed using Lipofectamine RNAiMAX Transfection Reagent (Invitrogen) according to the manufacturer's specifications.

### Confocal microscopy

Cells were fixed for 15 minutes with formalin and permeabilized for 5 minutes with 0.05% saponin in PEM buffer [80 mM PIPES, 5 mM EGTA, 1 mM MgCl<sub>2</sub> (pH 6.8)]. Primary antibodies were diluted in PBS supplemented with 0.05% saponin. Confocal images were acquired with a 100× objective on a Zeiss LSM 710 Meta confocal laser-scanning microscope.

### Reagents and antibodies

Hrs antibody has been previously described (Raiborg et al., 2001), Tsg101 antibody was purchased from Abcam (Cambridge, UK). Phosphorylated MRLC (MRLC-P) and total MRLC antibodies were purchased from Cell Signaling Technology (Danvers, MA). Vinculin antibody was purchased from Sigma, antibody against giantin from Covance. Rhodamine phalloidin (actin) was purchased from Molecular Probes (Invitrogen), and β-actin from Sigma. Mouse IgG conjugated to horseradish peroxidase (HRP), rabbit IgG-HRP and Cy2-, Cy3- and Cy5-conjugated secondary antibodies were purchased from Jackson ImmunoResearch Laboratories (Suffolk, UK). Tag-RFP-Vinculin was purchased from Evrogen (Moscow, Russia). Phosphomimetic human MRLC was a kind gift from Jongkyeong Chung (Seoul National University, South Korea). MLCK antibodies (Y471-P and total MLCK) were purchased from Santa Cruz Biotechnology, Inc (Santa Cruz).

### Live time-lapse microscopy

BJ cells were plated on glass-bottomed 35 mm MatTek dishes, grown to confluence and wounded with a 10 μL pipette tip. Cells were observed for a period of 10 hours using a Biostation IM(R) (Nikon). Cells were maintained at 37°C and 5% CO<sub>2</sub> in humidified air throughout the observation period. One picture was acquired every 15 minutes. The velocity of migration was determined using Image J software.

### Immunoprecipitation

Cells were lysed in lysis buffer (10 mM Tris-HCl pH 7.5, 150 mM NaCl, 0.5 mM EDTA, 0.5% NP40, protease and phosphatase inhibitor cocktails). Protein lysates were incubated with 1.5 μg MLCK antibody or IgG mouse for 1 hour at 4°C with constant rotation. Protein G magnetic beads (Invitrogen) were added and incubated for one further hour at 4°C with constant rotation. After washing, associated proteins were eluted by boiling at 95°C for 5 minutes in SDS-sample buffer, resolved by SDS-PAGE, and analyzed by western blotting.

### Cell culture

BJ human foreskin fibroblasts were routinely cultured in Quantum 333 medium at 37°C and 5% CO<sub>2</sub>. For experiments, BJ cells were seeded out in Dulbecco's modified Eagle's medium supplemented with 10% FCS and penicillin–streptomycin.

### Transient transfection

Vinculin-RFP was transfected into BJ cells with Fugene (Promega) according to the manufacturer's specifications. Cells were left to express the construct for 48 hours

before live confocal time-lapse microscopy was performed. Phosphomimetic MRLC was transfected into BJ cells using Lipofectamine Plus (Invitrogen) according to the manufacturer's specifications.

### Cell spreading assay

Coverslips were coated with fibronectin (20 μg/mL) overnight at 4°C and blocked with 10 mg/mL BSA for 30 minutes at room temperature. siRNA-depleted BJ fibroblasts were trypsinized, trypsin-inactivated, spun down and resuspended in serum-free medium. Cells were left to recover in the incubator for 10 minutes, and were seeded onto coverslips and allowed to adhere for 90 minutes (37°C, 5% CO<sub>2</sub>). Cells were subsequently washed, fixed and permeabilized. Cells were stained for actin in order to visualize the cells, and the surface area of cells was assessed using Zeiss LSM Image Examiner software.

### Confocal live-cell time-lapse microscopy

For confocal live-cell time-lapse recording, BJ cells expressing TagRFP-vinculin and depleted of endogenous HRS and TSG101 were plated on glass-bottomed 35 mm MatTek dishes. Complete Z stacks of transfected cells were recorded every minute for a period of 1 hour at 37°C under 5% CO<sub>2</sub> using a Zeiss LSM 510 LIVE confocal microscope.

## Acknowledgements

We thank Jongkyeong Chung for kindly providing a plasmid encoding a phosphomimetic mutant of human MRLC. V.H.L. is a PhD student of the Norwegian Cancer Society. V.H.L. wrote the article and performed experiments. H.S. supervised the study and edited the manuscript. Both authors agree with the final version of the manuscript.

## Funding

H.S. is the recipient of an Advanced Grant from the European Research Council [grant number GA 233146]. This work was also supported by the Research Council of Norway [grant number 179571/V40].

Supplementary material available online at

<http://jcs.biologists.org/lookup/suppl/doi:10.1242/jcs.088310/-/DC1>

## References

- Abercrombie, M., Heaysman, J. E. and Pegrum, S. M. (1970). The locomotion of fibroblasts in culture. I. Movements of the leading edge. *Exp. Cell Res.* **59**, 393-398.
- Arthur, W. T. and Burridge, K. (2001). RhoA inactivation by p190RhoGAP regulates cell spreading and migration by promoting membrane protrusion and polarity. *Mol. Biol. Cell* **12**, 2711-2720.
- Arthur, W. T., Petch, L. A. and Burridge, K. (2000). Integrin engagement suppresses RhoA activity via a c-Src-dependent mechanism. *Curr. Biol.* **10**, 719-722.
- Betapudi, V., Licate, L. S. and Egelhoff, T. T. (2006). Distinct roles of nonmuscle myosin II isoforms in the regulation of MDA-MB-231 breast cancer cell spreading and migration. *Cancer Res.* **66**, 4725-4733.
- Bhadriraju, K., Yang, M., Alom, Ruiz, S., Pirone, D., Tan, J. and Chen, C. S. (2007). Activation of ROCK by RhoA is regulated by cell adhesion, shape, and cytoskeletal tension. *Exp. Cell Res.* **313**, 3616-3623.
- Bisel, B., Wang, Y., Wei, J. H., Xiang, Y., Tang, D., Miron-Mendoza, M., Yoshimura, S., Nakamura, N. and Seemann, J. (2008). ERK regulates Golgi and centrosome orientation towards the leading edge through GRASP65. *J. Cell Biol.* **182**, 837-843.
- Chanut-Delalande, H., Jung, A. C., Lin, L., Baer, M. M., Bilstein, A., Cabernard, C., Leptin, M. and Affolter, M. (2007). A genetic mosaic analysis with a repressible cell marker screen to identify genes involved in tracheal cell migration during *Drosophila* air sac morphogenesis. *Genetics* **176**, 2177-2187.
- Chanut-Delalande, H., Jung, A. C., Baer, M. M., Lin, L., Payre, F. and Affolter, M. (2010). The Hrs/Stam complex acts as a positive and negative regulator of RTK signaling during *Drosophila* development. *PLoS ONE* **5**, e10245.
- Coll, J. L., Ben-Ze'ev, A., Ezzell, R. M., Rodriguez Fernandez, J. L., Baribault, H., Oshima, R. G. and Adamson, E. D. (1995). Targeted disruption of vinculin genes in F9 and embryonic stem cells changes cell morphology, adhesion, and locomotion. *Proc. Natl. Acad. Sci. USA* **92**, 9161-9165.
- Connell, L. E. and Helfman, D. M. (2006). Myosin light chain kinase plays a role in the regulation of epithelial cell survival. *J. Cell Sci.* **119**, 2269-2281.
- Crowley, E. and Horwitz, A. F. (1995). Tyrosine phosphorylation and cytoskeletal tension regulate the release of fibroblast adhesions. *J. Cell Biol.* **131**, 525-537.
- Etienne-Manneville, S. and Hall, A. (2001). Integrin-mediated activation of Cdc42 controls cell polarity in migrating astrocytes through PKC. *Cell* **106**, 489-498.
- Gomes, E. R., Jani, S. and Gundersen, G. G. (2005). Nuclear movement regulated by Cdc42, MRCK, myosin, and actin flow establishes MTOC polarization in migrating cells. *Cell* **121**, 451-463.

- Hakak, Y. and Martin, G. S.** (1999). Ubiquitin-dependent degradation of active Src. *Curr. Biol.* **9**, 1039-1042.
- Harris, K. F., Shoji, I., Cooper, E. M., Kumar, S., Oda, H. and Howley, P. M.** (1999). Ubiquitin-mediated degradation of active Src tyrosine kinase. *Proc. Natl. Acad. Sci. USA* **96**, 13738-13743.
- Hay, E. D.** (1981). Extracellular matrix. *J. Cell Biol.* **91**, 205s-223s.
- Howlett, C. J. and Robbins, S. M.** (2002). Membrane-anchored Cbl suppresses Hck protein-tyrosine kinase mediated cellular transformation. *Oncogene* **21**, 1707-1716.
- Huveneers, S. and Danen, E. H.** (2009). Adhesion signaling – crosstalk between integrins, Src and Rho. *J. Cell Sci.* **122**, 1059-1069.
- Hynes, R. O.** (1992). Integrins: versatility, modulation, and signaling in cell adhesion. *Cell* **69**, 11-25.
- Izzard, C. S. and Lochner, L. R.** (1980). Formation of cell-to-substrate contacts during fibroblast motility: an interference-reflexion study. *J. Cell Sci.* **42**, 81-116.
- Kim, M., Tezuka, T., Tanaka, K. and Yamamoto, T.** (2004). Cbl-c suppresses v-Src-induced transformation through ubiquitin-dependent protein degradation. *Oncogene* **23**, 1645-1655.
- Kupfer, A., Louvard, D. and Singer, S. J.** (1982). Polarization of the Golgi apparatus and the microtubule-organizing center in cultured fibroblasts at the edge of an experimental wound. *Proc. Natl. Acad. Sci. USA* **79**, 2603-2607.
- Lobert, V. H., Brech, A., Pedersen, N. M., Wesche, J., Oppelt, A., Malerod, L. and Stenmark, H.** (2010). Ubiquitination of alpha5beta1 integrin controls fibroblast migration through lysosomal degradation of fibronectin-integrin complexes. *Dev. Cell* **19**, 148-159.
- Miserey-Lenkei, S., Chalancon, G., Bardin, S., Formstecher, E., Goud, B. and Echard, A.** (2010). Rab and actomyosin-dependent fission of transport vesicles at the Golgi complex. *Nat. Cell Biol.* **12**, 645-654.
- Mitra, S. K., Hanson, D. A. and Schlaepfer, D. D.** (2005). Focal adhesion kinase: in command and control of cell motility. *Nat. Rev. Mol. Cell Biol.* **6**, 56-68.
- Moberg, K. H., Schelble, S., Burdick, S. K. and Hariharan, I. K.** (2005). Mutations in erupted, the *Drosophila* ortholog of mammalian tumor susceptibility gene 101, elicit non-cell-autonomous overgrowth. *Dev. Cell* **9**, 699-710.
- Paolini, R., Molfetta, R., Piccoli, M., Frati, L. and Santoni, A.** (2001). Ubiquitination and degradation of Syk and ZAP-70 protein tyrosine kinases in human NK cells upon CD16 engagement. *Proc. Natl. Acad. Sci. USA* **98**, 9611-9616.
- Raiborg, C., Bremnes, B., Mehlum, A., Gillooly, D. J., D'Arrigo, A., Stang, E. and Stenmark, H.** (2001). FYVE and coiled-coil domains determine the specific localisation of Hrs to early endosomes. *J. Cell Sci.* **114**, 2255-2263.
- Rodahl, L. M., Haglund, K., Sem-Jacobsen, C., Wendler, F., Vincent, J. P., Lindmo, K., Rusten, T. E. and Stenmark, H.** (2009). Disruption of Vps4 and JNK function in *Drosophila* causes tumour growth. *PLoS ONE* **4**, e4354.
- Saunders, R. M., Holt, M. R., Jennings, L., Sutton, D. H., Barsukov, I. L., Bobkov, A., Liddington, R. C., Adamson, E. A., Dunn, G. A. and Critchley, D. R.** (2006). Role of vinculin in regulating focal adhesion turnover. *Eur. J. Cell Biol.* **85**, 487-500.
- Sevrioukov, E. A., Moghrabi, N., Kuhn, M. and Kramer, H.** (2005). A mutation in dVps28 reveals a link between a subunit of the endosomal sorting complex required for transport-I complex and the actin cytoskeleton in *Drosophila*. *Mol. Biol. Cell* **16**, 2301-2312.
- Stuffers, S., Sem Wegner, C., Stenmark, H. and Brech, A.** (2009). Multivesicular endosome biogenesis in the absence of ESCRTs. *Traffic* **10**, 925-937.
- Takizawa, N., Ikebe, R., Ikebe, M. and Luna, E. J.** (2007). Supervillin slows cell spreading by facilitating myosin II activation at the cell periphery. *J. Cell Sci.* **120**, 3792-3803.
- Thompson, B. J., Mathieu, J., Sung, H. H., Loeser, E., Rorth, P. and Cohen, S. M.** (2005). Tumor suppressor properties of the ESCRT-II complex component Vps25 in *Drosophila*. *Dev. Cell* **9**, 711-720.
- Totsukawa, G., Wu, Y., Sasaki, Y., Hartshorne, D. J., Yamakita, Y., Yamashiro, S. and Matsumura, F.** (2004). Distinct roles of MLCK and ROCK in the regulation of membrane protrusions and focal adhesion dynamics during cell migration of fibroblasts. *J. Cell Biol.* **164**, 427-439.
- Tu, C., Ortega-Cava, C. F., Winograd, P., Stanton, M. J., Reddi, A. L., Dodge, I., Arya, R., Dimri, M., Clubb, R. J., Naramura, M. et al.** (2010). Endosomal-sorting complexes required for transport (ESCRT) pathway-dependent endosomal traffic regulates the localization of active Src at focal adhesions. *Proc. Natl. Acad. Sci. USA* **107**, 16107-16112.
- Vaccari, T. and Bilder, D.** (2005). The *Drosophila* tumor suppressor vps25 prevents nonautonomous overproliferation by regulating notch trafficking. *Dev. Cell* **9**, 687-698.
- Valderrama, F., Babia, T., Ayala, I., Kok, J. W., Renau-Piqueras, J. and Egea, G.** (1998). Actin microfilaments are essential for the cytoplasmic positioning and morphology of the Golgi complex. *Eur. J. Cell Biol.* **76**, 9-17.
- Valderrama, F., Duran, J. M., Babia, T., Barth, H., Renau-Piqueras, J. and Egea, G.** (2001). Actin microfilaments facilitate the retrograde transport from the Golgi complex to the endoplasmic reticulum in mammalian cells. *Traffic* **2**, 717-726.
- Vicente-Manzanares, M., Ma, X., Adelstein, R. S. and Horwitz, A. R.** (2009). Non-muscle myosin II takes centre stage in cell adhesion and migration. *Nat. Rev. Mol. Cell Biol.* **10**, 778-790.
- Webb, D. J., Parsons, J. T. and Horwitz, A. F.** (2002). Adhesion assembly, disassembly and turnover in migrating cells – over and over and over again. *Nat. Cell Biol.* **4**, E97-E100.
- Yokouchi, M., Kondo, T., Sanjay, A., Houghton, A., Yoshimura, A., Komiyama, S., Zhang, H. and Baron, R.** (2001). Src-catalyzed phosphorylation of c-Cbl leads to the interdependent ubiquitination of both proteins. *J. Biol. Chem.* **276**, 35185-35193.